Catalysis Today 164 (2011) 16–22

Contents lists available at ScienceDirect

Catalysis Today

journal homepage: www.elsevier.com/locate/cattod

Modeling of hydrogen vacancy for dissociative adsorption of H_2 on Pd (1 1 1) surface by a quantum chemical molecular dynamics

Farouq Ahmed[a], Md. Khorshed Alam[c], Ryuji Miura[c], Ai Suzuki[b], Hideyuki Tsuboi[a], Nozomu Hatakeyama[a], Akira Endou[a], Hiromitsu Takaba[c], Momoji Kubo[d], Akira Miyamoto[b,c,a,*]

[a] Department of Applied Chemistry, Graduate School of Engineering, Tohoku University, 6-6-10-205 Aoba, Sendai 980-8579, Japan
[b] New Industry Creation Hatchery Center, Tohoku University, 6-6-10-205 Aoba, Sendai 980-8579, Japan
[c] Department of Chemical Engineering, Graduate School of Engineering, Tohoku University, 6-6-10-205 Aoba, Sendai 980-8579, Japan
[d] Fracture and Reliability Research Institute, Graduate School of Engineering, Tohoku University, 6-6-11-701 Aoba, Sendai 980-8579, Japan

ARTICLE INFO

Article history:
Available online 28 October 2010

Keywords:
UA-QCMD
Influence of surface hydrogen vacancy
Hydrogen dissociative adsorption

ABSTRACT

In this article modeling of dissociative adsorption of hydrogen on Pd (1 1 1) surface by ultra-accelerated quantum chemical molecular dynamics (UA-QCMD) was reported for the better understanding of the role of hydrogen vacancy for the dissociative adsorption of hydrogen. Here we have demonstrated and examined the isolated steps of hydrogen dissociative adsorption on Pd (1 1 1) surface. The direct observations of dissociative adsorption of hydrogen on Pd (1 1 1) surface (different vacancy models) were successfully simulated. From the analysis of the change of electronic structures and the dynamics of dissociative adsorption process, we can conclude that divacancy sites are inactive for dissociative adsorption of hydrogen on Pd (1 1 1) surface. Our findings suggest that H_2 dissociation on Pd (1 1 1) requires an ensemble of at least three hydrogen vacancies.

Our results support the original interpretation of STM work of Mitsui et al. that three or more hydrogen vacancy is required for dissociative adsorption of hydrogen.

© 2010 Elsevier B.V. All rights reserved.

1. Introduction

Understanding the fundamental mechanisms that govern the behavior of hydrogen on surfaces is important to new technologies involving hydrogen production, storage, and energy conversion [1–4]. Simultaneously, the dissociative adsorption of molecules is a crucial reaction step in most catalytic processes at various surfaces. In particular, the interaction of hydrogen with transition metal surfaces has served as a model system for the study of elementary reaction steps in the dissociation dynamics experimentally and theoretically [5–8]. Focusing the attention on the specific systems considered here, hydrogen on Pd (1 1 1) surface, several experimental [9–11] and theoretical [12–19] studies can be found in the literature.

It has been generally accepted that the dissociative adsorption of the diatomic molecule H_2 is to require at least two adjacent and empty atomic adsorption sites or vacancies based on early studies of Conrad et al. [20] and Langmuir [21]. The creation of active sites for H_2 dissociation will thus involve the formation of individual vacancies and their subsequent diffusion and aggregation [22]. In a recent STM work, Mitsui et al. [10] studied the formation of ordered hydrogen layers on Pd (1 1 1) surface. In contrast very interestingly, they found that hydrogen molecules impinging on an almost hydrogen saturated Pd (1 1 1) surface did not adsorb in divacancy (2V) sites. Indeed, Mitsui et al. [10] have found that near saturation coverage, for the facile molecular dissociation on Pd (1 1 1) surface requires three or more assembling vacancy sites of H atoms.

Later on Lopez et al. [23] reported that a Pd atom not directly bound to H is needed to promote dissociation, so that clusters of at least three vacancies (3V) are required. To verify the study of Mitsui et al. [10], Giordano et al. [24] provided a quantitative theoretical support to this interpretation by performing *ab initio* calculations of the typical kinetic barriers for both isolated H vacancies and H divacancies on hydrogen-covered Pd (1 1 1). They found that the quantum wave nature of hydrogen fully accounts for the threefold appearance of the 2V in STM even in the absence of thermal fluctuations. Sungho et al. [25] determined the ground-state structure of divacancies in a hydrogen monolayer on the Pd (1 1 1) surface. They found that a hydrogen atom in a 2V defect experiences significant quantum effects and that the ground-state wave function is centered at the hcp site rather than the fcc site normally occupied by H atoms on Pd (1 1 1).

* Corresponding author at: Department of Chemical Engineering, Graduate School of Engineering, Tohoku University, 6-6-10-205 Aoba, Sendai 980-8579, Japan. Tel.: +81 22 795 7233; fax: +81 22 795 7235.
E-mail addresses: farouq80@yahoo.com (F. Ahmed), miyamoto@aki.che.tohoku.ac.jp (A. Miyamoto).

0920-5861/$ – see front matter © 2010 Elsevier B.V. All rights reserved.
doi:10.1016/j.cattod.2010.10.009

Above findings [10,11,23–25] led to speculations that the accepted notion that 2V sites are required for the dissociative adsorption of diatomic molecules might not be correct and too simple to explain the dissociative adsorption of hydrogen on Pd (1 1 1) surface. But very recently, based on *ab initio* molecular dynamics (AIMD) trajectories, Groß and Dianat [26] unambiguously demonstrated that 2V is still sufficient (supporting Conrad et al. [20] and Langmuir [21] study) to dissociate hydrogen molecules provided that the kinetic energy of the incident molecules is large enough to overcome the relatively small energy barrier.

Despite continued investigations and researches, the mechanistic details of dissociative adsorption of hydrogen are still illusive. New theoretical work attempting to understand the coverage effects in activation barriers and, perhaps, the dynamics of dissociation and comparison of change of the electronic structures are necessary to elucidate actual mechanism. In that study, we introduce UA-QCMD simulator as a tool for the quantitative determination of the role of hydrogen vacancy for the dissociative adsorption of hydrogen on Pd (1 1 1) surface.

2. Computational methods

2.1. Quantum chemical molecular dynamics method

We used our in-house code UA-QCMD [27–29] to investigate the electronic and structural changes as well as diffusion characteristics of H_2 on the surface of metal catalyst Pd (1 1 1) surface under periodic boundary condition. UA-QCMD enables one to perform quantum chemical molecular dynamics calculation by reflecting binding energy and atomic charges based on quantum chemistry calculations. Calculation of the electronic structure based on quantum chemistry was performed by tight binding quantum chemical molecular dynamics code (TB-QC), *New-Colors* [27–29]. The accuracy of the method is calibrated to reproduce a limited set of first-principles calculation results and is able to interpolate between different structures, at a cost which is orders of magnitude less than that required to do by first principle calculations on the same systems. The parameterized TB-QC method is inherently faster than first principle methods because it has a smaller equation and does not need a self-consistency step once the parameters have been fitted. This method has been tested on all transition metals and found to produce elastic constants, vacancy formation energies and surface energies are in very good agreement with first-principle calculations and experiment [30–36]. A single point TB-QC calculation was performed, and the atomic charges and Morse-type 2-body interatomic potentials were updated at intervals during MD simulation. After dynamics calculation, again this model was transferred for a single point TB-QC calculation and resumed the MD simulation. A different step of molecular dynamics calculation was performed with an integration time step of 0.1 fs.

2.2. First-principle parameterization in tight-binding calculation

In order to set the Hamiltonian matrix **H** and overlap integral matrix **S** in our TB-QC simulator which is a part of our UA-QCMD simulator, exponents of a Slater-type atomic orbital (AO), denoted as ζ_r, and valence state ionization potentials (VSIPs) for the 1*s* AO of H atoms, 4*p* and 4*d* AOs of Pd atoms are necessary. The former parameters are used to calculate the **S** matrix and H_{rs} in Eq. (1). The latter ones are used for the diagonal element of H (H_{rr} or H_{ss} in Eq. (1)). The relationship between H_{rr} and VSIP of rth AO of the ith atom ($I^i{}_r$) is described as $H_{rr} = -I^i{}_r$. In our UA-QCMD simulator, these are represented by the polynomial functions of atomic charges. The ζ_r, and H_{rr} are calculated by the polynomial functions of atomic charges described by Eqs. (1) and (2), respectively.

$$\zeta_r = a_0 + \sum_{k=1}^{5} a_k (Z_i)^k \tag{1}$$

$$H_{rr} = b_0 + \sum_{k=1}^{5} b_k (Z_i)^k \tag{2}$$

In Eqs. (1) and (2), Z_i corresponds to the atomic charge on the atom i. The parameters regarding ζ_r, i.e., a_0, a_1, a_2, a_3, a_4, and a_5 in Eq. (1) and regarding H_{rr}, i.e., b_0, b_1, b_2, b_3, b_4, and b_5 in Eq. (2), were determined so as to reproduce the binding energies and electronic structures of a H_2/Pd (1 1 1) surface model was obtained by density functional theory (DFT) calculations, which are summarized in Tables 1 and 2, respectively and will be explained later on.

2.3. Periodic density functional theory method

The DFT calculations were also performed in order to validate the accuracy of our TB-QC method. The DMol [3] code [37] was used for the present purpose and double numerical basis sets with polarization functions (DNP) were employed. The geometry optimization was performed using the Vosko, Wilk, and Nusair (VWN) local density approximation functional [38], while the energies were recalculated using the generalized gradient approximation (GGA) with Perdew–Burke–Ernzerhof (PBE) exchange-correlation functional [39] was adopted for energy calculations. The charge population was analyzed by Hirshfeld method. Binding energies, E_{bind} described by Eq. (3), were calculated as energy difference between the total energy of optimized H_2/H/Pd system and the summation of total energies of individual atom present in the system. In Eq. (3) A and B refer total number of, H atoms, and Pd atoms, respectively for different Pd surface models. Adsorption energies, E_{ads} described by Eq. (4), were calculated as energy difference between the total energy of optimized H_2/H/Pd system and the summation of total energies of isolated H/Pd surface and H_2 molecule.

$$E_{bind} = E_{H_2/H/Pd} - (A \cdot E_H + B \cdot E_{Pd}) \tag{3}$$

$$E_{ads} = E_{H_2/H/Pd} - (E_{H/Pd} + E_{H_2}) \tag{4}$$

2.4. Model preparation

In order to validate our parameters shown in Tables 1 and 2, a bulk model of Pd cluster containing 32 atoms was prepared, which was depicted in Fig. 1a. The influence of the surface hydrogen vacancy was simulated applying the UA-QCMD to a target model of H_2/Pd (1 1 1) catalyst surface, which is shown in Fig. 1b. The surface was modeled by a slab of three layers for the Pd (1 1 1) surface within (2×2) unit cells using a Monkhorst–Pack grid of $(5 \times 5 \times 1)$ k-points. The Pd (1 1 1) surface model consists of 96 Pd atoms in the unit cell. In the present study, the Pd (1 1 1) surface containing 25 dissociated hydrogen atoms was modeled. Hydrogen atoms were included in Pd cluster as adsorbed hydrogens in 3 fold fcc sites to represent the reduced condition. The initial lateral positions and orientations of the H_2 molecule were chosen randomly. Three-dimensional periodic boundary condition was applied in the unit cells. A hydrogen molecule was placed in the vacuum region of the unit cells. The dynamics simulations were started with an initial distance of 7.13 Å between the hydrogen molecule and the top layer of Pd (1 1 1) surface, which initial distance is enough to ignore interactions between the hydrogen molecule and the surfaces. The specified kinetic energies of the center of mass of the hydrogen molecule was given between 0.02 and 0.13 eV along to the direction to the surfaces that corresponds to a velocity of 4000–5000 m/s.

Table 1
Determined coefficient of a single ζ parameter in a Slater-type atomic orbital. Coefficients a_0, a_1, a_2, a_3, a_4, and a_5 used in Eq. (1).

Element	AO	b_0	b_1	b_2	b_3	b_4	b_5
H	*s*	−6.2010	−17.8700	0.000	0.000	0.0	0.0000
Pd	*s*	−5.4000	−7.4574	0.000	0.000	0.000	0.000
	p	−2.9000	−0.5000	0.000	0.000	0.000	0.000
	d	−9.0000	−2.1314	0.000	0.000	0.000	0.000

Table 2
Determined coefficient parameter of H_{rr} parameter. Coefficients b_0, b_1, b_2, b_3, b_4, and b_5 used in Eq. (2).

Element	AO	a_0	a_1	a_2	a_3	a_4	a_5
H	*s*	0.9484	1.5794	0.000	0.000	0.000	0.000
Pd	*s*	2.0000	4.4211	0.0000	0.000	0.000	0.000
	p	1.9000	5.2163	0.0000	0.000	0.000	0.000
	d	2.6000	2.6810	0.0000	0.000	0.000	0.000

Velocity of hydrogen was determined from Maxwell–Boltzmann distribution of speeds at 573 K.

3. Results and discussion

3.1. Validation of parameters used in the UA-QCMD method

Validation was carried out by comparison of the electronic properties obtained by DFT with that of TB-QC method. Pd bulk model (Fig. 1a) was used for validation of Pd parameters listed in Tables 1 and 2.

The accuracy of the used parameters were checked by the comparison of the atomic charges, atomic orbital populations, bond populations, and total binding energies of the Pd bulk model obtained by DFT (with different exchange correlation potentials) and TB-QC method. Comparison of the atomic charges of Pd atoms by TB-QC (0.001) and DFT (0.00), we could clarify that the atomic charges of Pd atoms were close to those obtained by DFT. Comparison of the bond populations of Pd–Pd in Pd bulk model calculated by TB-QC (0.11) agreed well with those by DFT (0.09) results. Table 3 compares the ratios of the atomic orbital populations for individual atoms obtained by DFT and TB-QC method. This table shows

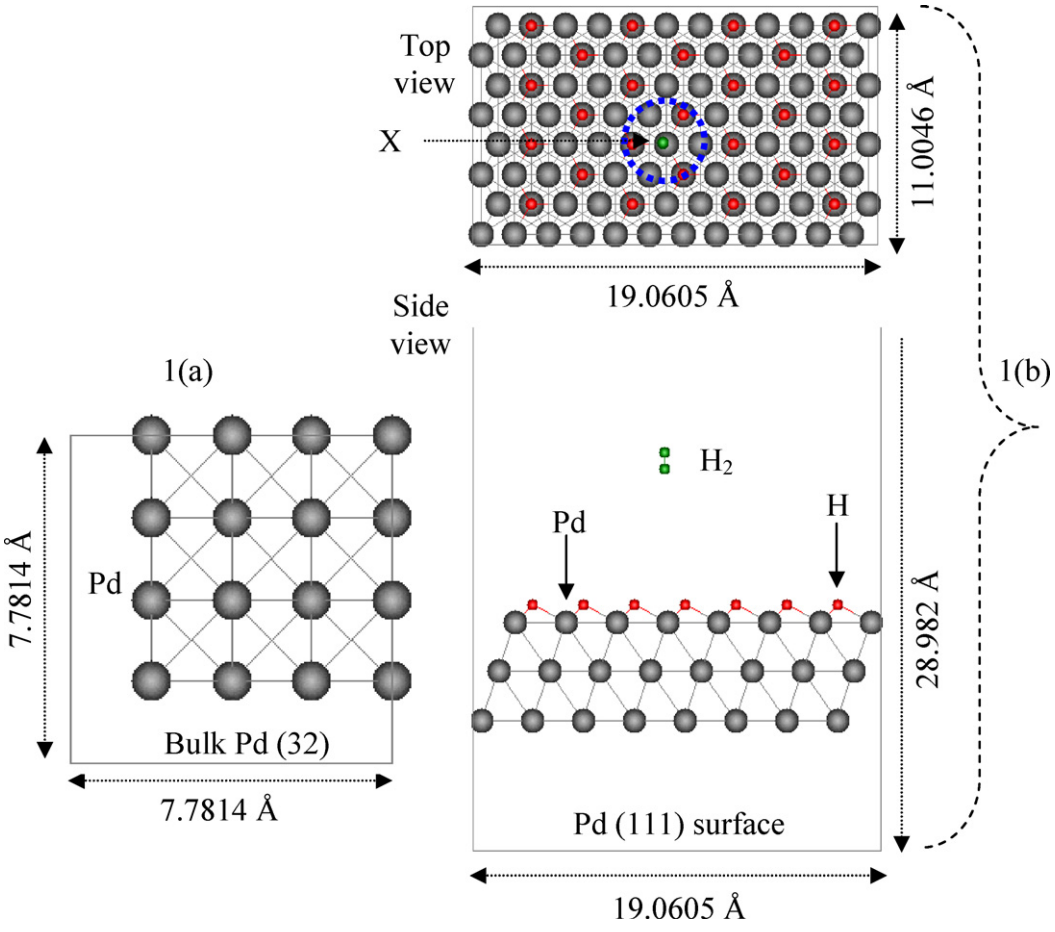

Fig. 1. (a) Pd bulk model (cell parameters: $a = 7.784$ Å, $b = 7.784$ Å, $c = 7.784$ Å, and $\alpha = \beta = \gamma = 90^\circ$) was used in the validation of parameterization and (b) model for Pd (1 1 1) surface (cell parameters: $a = 19.0605$ Å, $b = 11.0046$ Å, $c = 28.982$ Å, and $\alpha = \beta = \gamma = 90^\circ$) was used in the UA-QCMD simulation. Adsorbed hydrogen denoted red in color and molecular hydrogen denoted as green. In (b), X denotes the position where hydrogen adsorbed. (For interpretation of the references to color in this figure legend, the reader is referred to the web version of this article.)

Table 3
Comparison of atomic orbital populations of Pd bulk (32 atoms) model obtained by DFT and TB-QC method.

Method	*s*%	*p*%	*d*%
DFT	5.5	2.4	92.1
TB-QC	7.5	1.5	91.0

that atomic orbital ratios obtained by TB-QC were close to those obtained by DFT. Total binding energy of the bulk model obtained by DFT (−2764.52 kcal/mol) also shows good agreement with that of TB-QC (−2725.41 kcal/mol).

A top and side view of Pd (1 1 1) surface model was shown in Fig. 1b. Five different surface vacancy models are shown in Fig. 2a–e. The model that was used for quantum chemical molecular dynamics calculation consists of three layers of Pd atoms. Only the first layer of Pd was pre-covered with adsorbed hydrogen atoms and the vacancies were also present on that first layer. To calculate total binding energy of those saturated and vacancy models, only 1st layer Pd atoms were considered because contribution of remaining 2nd and 3rd layers was considered as similar effect in five different models. This procedure was also helps to reduce computational cost in DFT calculation. Validation calculations of Pd and H parameters listed in Tables 1 and 2 were carried out by TB-QC method using surface model consists of several H atoms (Fig. 1b). Total binding energies of the five different vacancy models of Pd (1 1 1) surface obtained by DFT and TB-QC methods were compared. Table 4 showing the reasonable agreement between the energies obtained by two different methods. To find out the interaction energy between Pd and H at the adsorbed state, we carried out the calculation of bond energies of diatomic molecule (D_{AB}) for H–H, and Pd–H bond pairs, which is shown in Table 5. It was shown that the results obtained by TB-QC method agreed well with those obtained by DFT and experimental method [40].

3.2. Adsorption of H on Pd surfaces

The dissociative adsorption of H_2 was simulated applying the UA-QCMD to a target model of Pd (1 1 1) surfaces. Our UA-QCMD results also showed that three fold fcc-hollow site was the stable adsorption site for hydrogen atom on Pd (1 1 1) surface where the Pd–H distance is from 1.78 Å to 1.8 Å, which corresponds to a vertical height of 0.80–0.85 Å of H above the surface. The calculated adsorption energies of hydrogen atom in different adsorption sites are summarized in Table 6. In agreement with earlier low-energy diffraction studies [7] and total-energy calculations [8,9], we have found that H atoms adsorb strongly on the three-fold face-centered cubic (fcc) sites.

3.3. Dynamics of dissociative adsorption process of hydrogen molecule on different vacancy sites of H atoms on Pd (1 1 1) surfaces

Five different calculation models were prepared on the basis of surface hydrogen vacancy to investigate the influence of surface hydrogen vacancy for the dissociative adsorption of hydrogen on Pd (1 1 1) surface, which is shown in Fig. 2.

3.3.1. Saturated surface (0V)

Fig. 2a represents the saturated surface, which was fully covered with 25 adsorbed H atoms. Snapshot at 0 fs represents the initial position of H_2 molecule above the Pd (1 1 1) surface. Snapshot at 140 fs represents the H_2 molecule approached to the Pd (1 1 1) surface perpendicularly. Finally, the snapshot at 280 fs shows that H_2 molecule without adsorbing on the surface departed from the surface.

3.3.2. Divacancy surface (2V)

Similarly in Fig. 2b the snapshot at 0 fs represents the initial position of H_2 molecule and the snapshot at 153 fs shows that molecular hydrogen approached to the Pd (1 1 1) surface perpendicularly. Finally, snapshot at 165 fs shows that H_2 molecule adsorbed on the surface in molecular form. This result is contrary to Langmuir [21] assumption that two hydrogen vacancies are sufficient for the dissociative adsorption of hydrogen. Here the bond length between H–H remains unchanged (0.75 Å) after adsorption on Pd (1 1 1) surface. We could not observe any dissociation of H–H bond on the divacancy sites of Pd (1 1 1) surface. Here in divacancy sites only molecular adsorption occurs at 165 fs. It may be assumed that if we increase the simulation time more than 165 fs hydrogen may dissociate but usually it did not happen in our simulation. In that regards we continued our simulation up to 5000 fs to observe whether dissociative adsorption of hydrogen occurs or not but dissociation was not observed.

3.3.3. Trivacancy surface (3V)

In addition, we have investigated adsorption of hydrogen molecule on trivacancy sites of Pd (1 1 1) surface. In Fig. 2c snapshot at 162 fs shows that the hydrogen approached to the Pd (1 1 1) surface in parallel directions whereas it was in perpendicular direction incase of saturated and divacancy surfaces. Finally, snapshot at 562 fs we observed that hydrogen dissociatively adsorbed on the Pd (1 1 1) surface. Here bond length of H–H became 1.01 Å, whereas initial bond length was 0.75 Å, confirming the experimental findings by Mitsui et al. [10]. In that case H–H bond energy becomes 252.43 kJ/mol whereas initial bond energy was 440.11 kJ/mol.

3.3.4. Tetra- and pentavacancy (4V and 5V)

In Fig. 2d and e similar molecular dynamics calculations were performed on tetra- (4V) and penta- (5V) hydrogen vacancy sites, respectively, which was also confirms the dissociative adsorption of hydrogen on Pd (1 1 1) surface. In case of 4V surface H_2 molecule dissociatively adsorbed on the Pd (1 1 1) surface at 432 fs whereas in case of 5V surface it was dissociatively adsorbed on the surface at 348 fs.

From the inspection of the data analysis compared with the result obtained by different vacancy surfaces, we may suggest that the increase of hydrogen vacancies promotes the dissociative adsorption. Here as the surface hydrogen vacancy increases, dissociative adsorption time (the time needed for the dissociation of H_2 from the initial time of simulation) decreases (Table 7). This result qualitatively supports the STM study of Mitsui et al. [10] where hydrogen adsorption was frequently observed for trivacancy surface to larger vacancy surface.

In this article we have demonstrated a few snapshots, which show the important steps of molecular dynamics simulation. Specially to check divacancies can dissociate hydrogen molecule or not, simulations were carried out using different initial positions of hydrogen molecule and moreover fixing hydrogen vacancies in different positions. Ideally we have to check many points as initial starting points of molecular dynamics simulation. But in this article we have concentrate on two initial starting points to understand the effect of the location of deposited hydrogen molecule in dissociative adsorption process. Even though these two particular starting points are not sufficient to understand the whole mechanism but gives us some specific information to reveal interesting features of the initial starting points. From the simulation results of different conformations and positions we could find that hydrogen only molecularly adsorbed on the divacancy surface.

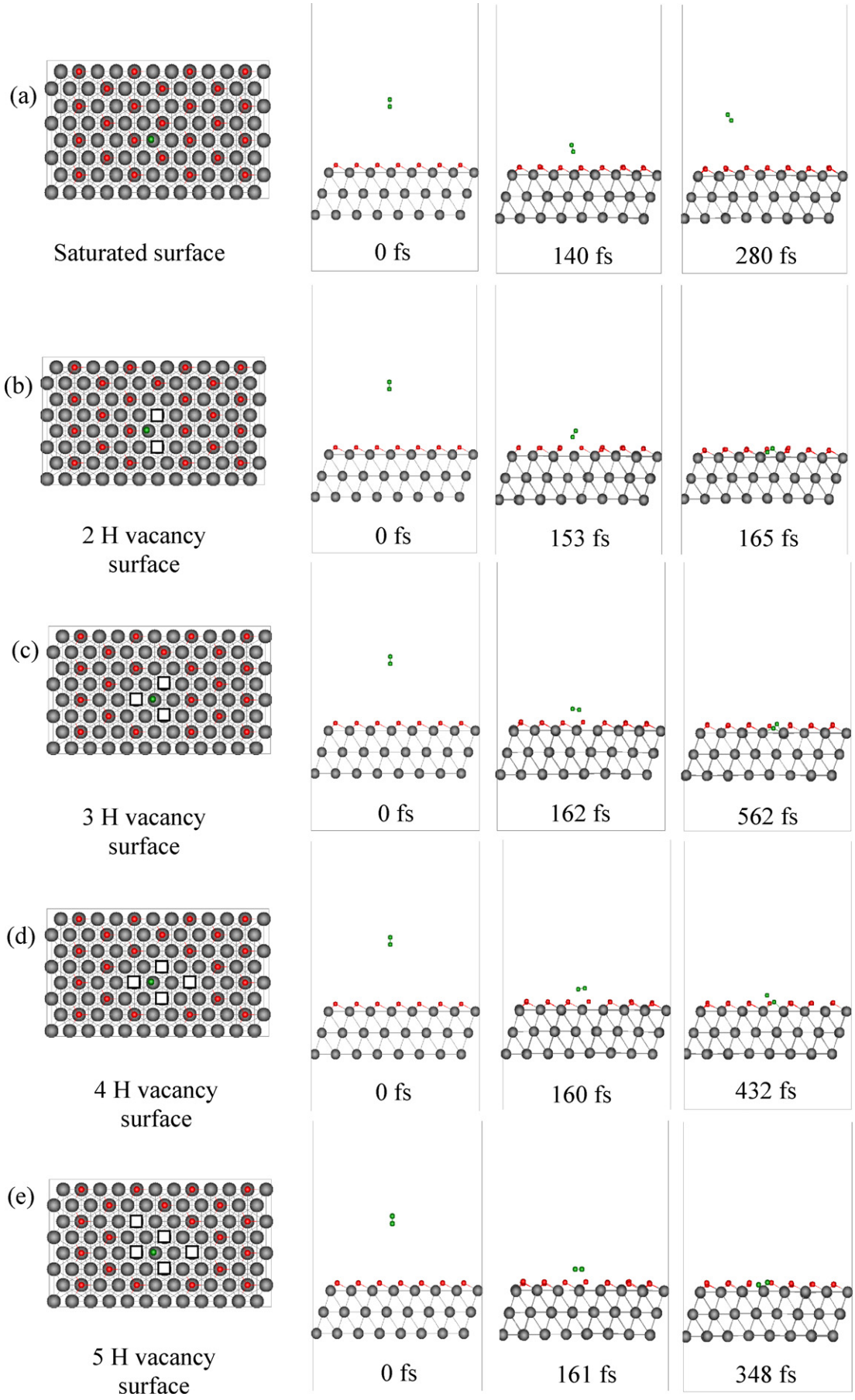

Fig. 2. Represents the snapshots of dynamics of dissociative adsorption process of H_2 on saturated and different vacancy surfaces of Pd (1 1 1).

Table 4
Comparison of total binding energy (kJ/mol) obtained by DFT and TB-QC method (first layer of surface model).

Method	Saturated	2V	3V	4V	5V
DFT	−3680.2	−3547.3	−3484.1	−3420.3	−3355.3
TB-QC optimized	−3689.4	−3652.2	−3544.5	−3524.1	−3441.1

Table 5
Comparison of bonding energies (D_{AB}) for diatomic molecule H–H and Pd–H, pairs obtained by DFT, TB-QC and experimental results.

Bond pair	Bond length (Å)	Bonding energy (D_{AB}) obtained by DFT (GGA/PBE) (kJ/mol)	Bonding energy (D_{AB}) obtained by TB-QC (kJ/mol)	Bonding energy (D_{AB}) obtained by experiment (kJ/mol)
H–H	0.74	−438.85	−439.02	−431.79
Pd–H	1.60	−294.52	−287.70	−282.04

Table 6
Adsorption energy (kJ/mol) of H_2 on five different adsorption sites of Pd (1 1 1) clean surface.

Adsorption energy (kJ/mol)				
On top	Bridge	fcc hollow site	hcp hollow site	Subsurface site
−9.69	−63.49	−134.30	−118.46	−164.23

Table 7
Comparison of dissociative adsorption time (fs) for five different vacancy surfaces.

Adsorption time (fs)				
Saturated (0V)	2V	3V	4V	5V
No adsorption	Molecular adsorption165	562	423	348

3.4. Effect of initial kinetic energy of H_2 deposition on Pd (1 1 1) surface

In order to check whether the divacancies can accommodate any H_2 molecule at all, we increases initial velocity of hydrogen molecule to 5000 m/s (0.13 eV) instead of 4000 m/s (0.02 eV), so that the small energy barrier found for H_2/Pd (1 1 1) surface at that coverage could be overcome [26]. Using kinetic energy about 0.02 eV, initially the H_2 molecule exists almost perpendicular to the surface but the molecule was so slow that the forces acting upon it cannot reorient the molecule. Here hydrogen molecule cannot changes its direction and then follows a molecular adsorption path. Using high initial kinetic energy, the molecule starts to rotate with a parallel direction to the surface. However, the molecule is so fast that it hits the repulsive region of the potential before it is in a favorable configuration to dissociative adsorption, hence molecular adsorption occurs. The activation barriers for the perpendicular orientation (with respect to H_2 with Pd (1 1 1) surface) were always much higher than those for the parallel orientation, which indicates that the parallel orientation is favored for H_2 dissociative adsorption [41]. In Fig. 2c–e initially H_2 was in a nonparallel orientation with respect to Pd (1 1 1) surface. But as the simulation proceeds it tends to reorient itself to achieve a parallel orientation and hence dissociatively adsorbed on the surface. For a low initial kinetic energy of 0.02 eV, which roughly corresponds to the kinetic energies of the H_2 molecules in the experiment [12], we did not observe any single dissociative adsorption event on the almost hydrogen-covered Pd (1 1 1) surface, thus confirming the experimental findings. Even though in 2V surface, using high initial kinetic energy (0.13 eV instead of 0.02 eV), to evaluate the results of Groß and Dianat [26], we could not find any dissociative adsorption of hydrogen molecule on the Pd (1 1 1) surface. Hence again confirming the experimental findings of Mitsui et al. [10] using both low and high initial kinetic energy.

3.5. Analysis of electronic structures

Table 8 shows the average atomic charges of first layer consisting of 32 Pd atoms and atomic charges of directly interacting Pd atom with respect to H_2 molecule (before and after adsorption) on the Pd (1 1 1) surface. Here as the number of surface hydrogen vacancies increases, atomic charge of Pd atoms also negatively increases (both in gas phase and adsorbed state). Here one interesting speculation is why Pd charge remains almost unchanged (before and after adsorption of H_2 molecule on the Pd surface) during the simulation (Table 8). It may suggest that donation–back donation makes the atomic charges of Pd atoms remain unchanged during the simulation. In this step the hydrogen molecule parallel in respect to the surface, which correspond to a more favorable configuration for electron transfer and the H–H bond length enlarged. From this explanation we may assume that as the simulation proceeds electron transferred from the molecular hydrogen to the Pd surface. According to above results it may also suggest that back donation may happen on hydrogen atom.

Table 8
Comparison of atomic charges of the first layer Pd atoms and interacting Pd atom with attacking hydrogen molecule (before and after adsorption of hydrogen molecule).

Average atomic charges on	Position of hydrogen molecule	Atomic charges				
		Saturated	2V	3V	4V	5V
First layer Pd atom	Before adsorption	−0.003	−0.006	−0.01	−0.012	−0.014
	After Adsorption	−0.006	−0.007	−0.01	−0.012	−0.014
Interacting Pd atom	Before adsorption	0.0162	−0.0265	−0.04	−0.042	−0.0454
	After Adsorption	0.0207	0.0341	0.0005	0.0009	−0.0133

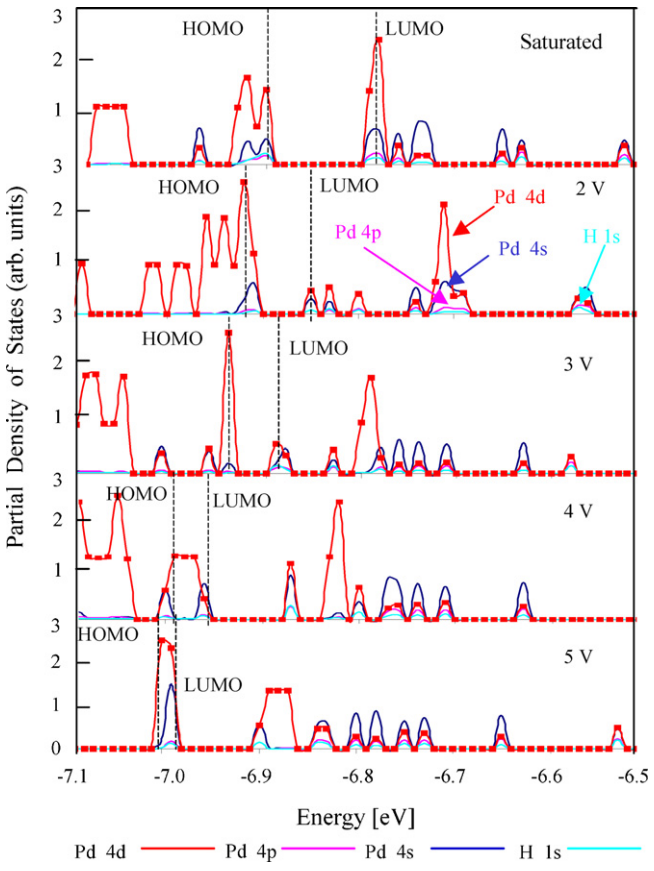

Fig. 3. Comparison of the partial density of states (PDOS) of five different vacancy surfaces.

Fig. 3 shows the partial density of states (PDOS) of five different vacancy models. The region between the top of the valance band (the HOMO in the molecules) and the conduction band (the LUMO in the molecules) is related to the reactivity: the system with a small band gap (HOMO–LUMO) is more reactive than that with a high value [42]. Here from the PDOS, at the adsorbed state of hydrogen molecule on the Pd (1 1 1) surface, it was found that the largest energy gap was observed for the saturated surface model. It was also found that as the hydrogen vacancy increases, the HOMO–LUMO energy levels shifted to the lower energy states. The band gap can serve as a measure of the excitability of the electron transfer: the smaller the energy gap, the easier to electron transfer and hence strong interaction between metal–hydrogen. As a result dissociative adsorption would occur more frequently in case of vacancy surfaces.

4. Concluding remarks

In this article, based on a line of theoretical studies involving quantum chemical molecular dynamics (QCMD), we have demonstrated and examined the isolated steps of hydrogen dissociative adsorption on Pd (1 1 1) surface and the influence of a surface hydrogen vacancy for the dissociative adsorption of hydrogen. The direct observations of dissociative adsorption of hydrogen on Pd (1 1 1) surfaces (different vacancy models) were successfully simulated. From the analysis of the change of electronic structures and the dynamics of dissociative adsorption, we can conclude that divacancies are inactive for dissociative adsorption of hydrogen on Pd (1 1 1) surface. Our findings suggest that H_2 dissociation on Pd (1 1 1) requires an ensemble of at least three hydrogen vacancies.

Our results support the original interpretation of STM work by Mitsui et al. [10] that two-vacancy sites seem inactive and that aggregates of three or more hydrogen vacancies are required for efficient H_2 dissociation.

References

[1] G.W. Huber, J.W. Shabaker, J.A. Dumesic, Science 300 (2003) 2075.
[2] L. Schlapbach, A. Züttel, Nature 414 (2001) 353.
[3] B.C.H. Steele, A. Heinzel, Nature 414 (2001) 345.
[4] S.G. Chalk, J.F. Miller, F.W. Wagner, J. Power Sources 86 (2000) 40.
[5] G.-J. Kroes, A. Groß, E.J. Baerends, M. Scheffler, D.A. McCormack, Acc. Chem. Res. 35 (2002) 193.
[6] A. Groß, M. Scheffler, Phys. Rev. B 57 (1998) 2493.
[7] D. Wetzig, M. Rutkowski, H. Zacharias, A. Groß, Phys. Rev. B 63 (2001) 205412.
[8] P. Nieto, et al., Science 312 (2006) 86.
[9] T.E. Felter, E.C. Sowa, M.A. Van Hove, Phys. Rev. B 40 (1989) 891.
[10] T. Mitsui, M.K. Rose, E. Fomin, D.F. Ogletree, M. Salmeron, Nature 422 (2003) 705.
[11] T. Mitsui, M.K. Rose, E. Fomin, D.F. Ogletree, M. Salmeron, Surf. Sci. 540 (2003) 5.
[12] W. Dong, G. Kresse, J. Furthmüller, J. Hafner, Phys. Rev. B 54 (1996) 2157.
[13] J.-F. Paul, P. Sautet, Phys. Rev. B 53 (1996) 8015.
[14] W. Dong, J. Hafner, Phys. Rev. B 56 (1997) 15396.
[15] R.A. Olsen, P.H.T. Philipsen, E.J. Baerends, G.J. Kroes, O.M. Løvvik, J. Chem. Phys. 106 (1997) 9286.
[16] O.M. Løvvik, R.A. Olsen, Phys. Rev. B 58 (1998) 10890.
[17] G.W. Watson, R.P.K. Wells, D.J. Willock, G.J. Hutchings, J. Phys. Chem. B 105 (2001) 4889.
[18] H.F. Busnengo, E. Pijper, G.J. Kroes, A. Salin, J. Chem. Phys. 119 (2003) 12553.
[19] I. Nikitin, W. Dong, H.F. Busnengo, A. Salin, Surf. Sci. 547 (2003) 149.
[20] H. Conrad, G. Ertl, E.E. Latta, Surf. Sci. 41 (1974) 435.
[21] I. Langmuir, J. Am. Chem. Soc. 38 (1916) 1145.
[22] H.S. Taylor, Theory of the catalytic surface, Proc. R. Soc. Lond. A 108 (1925) 105.
[23] N. Lopez, Z. Lodziana, F. Illas, M. Salmeron, Phys. Rev. Lett. 93 (2004) 146103.
[24] L. Giordano, L.D. Piazza, M. Trioni, F. Montalenti, Chem. Phys. Lett. 400 (2004) 163.
[25] K. Sungho, K. Seong-Gon, S.C. Erwin, Phys. Rev. B 76 (2007) 214109.
[26] A. Groß, A. Dianat, Phys. Rev. Lett. 98 (2007) 206107.
[27] F. Ahmed, Md.K. Alam, A. Suzuki, H. Tsuboi, K. Michihisa, N. Hatakeyama, A. Endou, H. Takaba, C.A. Del Carpio, M. Kubo, A. Miyamoto, J. Phys. Chem. C 113 (2009) 15676.
[28] Md.K. Alam, F. Ahmed, K. Nakamura, A. Suzuki, R. Sahnoun, H. Tsuboi, K. Michihisa, N. Hatakeyama, A. Endou, H. Takaba, C.A. Del Carpio, M. Kubo, A. Miyamoto, J. Phys. Chem. C 113 (2009) 7723.
[29] F. Ahmed, Md.K. Alam, A. Suzuki, H. Tsuboi, K. Michihisa, N. Hatakeyama, A. Endou, H. Takaba, C.A. Del Carpio, M. Kubo, A. Miyamoto, Appl. Surf. Sci. 256 (2010) 7643.
[30] M. Elanany, P. Selvam, T. Yokosuka, S. Takami, M. Kubo, A. Imamura, A. Miyamoto, J. Phys. Chem. B 107 (2003) 1518.
[31] Y. Luo, Y. Ito, H. Zhong, A. Endou, M. Kubo, S. Manogaran, A. Imamura, A. Miyamoto, Chem. Phys. Lett. 384 (2004) 30.
[32] R. Ishimoto, C. Jung, H. Tsuboi, M. Koyama, A. Endou, M. Kubo, C.A. Del Carpio, A. Miyamoto, Appl. Catal. A 305 (2006) 64.
[33] K. Kasahara, H. Tsuboi, M. Koyama, A. Endou, M. Kubo, C.A. Del Carpio, A. Miyamoto, Electrochem. Solid State Lett. 9 (2006) 490.
[34] P. Selvam, H. Tsuboi, M. Koyama, A. Endou, H. Takaba, M. Kubo, C.A. Del Carpio, A. Miyamoto, Rev. Chem. Eng. 22 (2006) 377.
[35] A. Endou, T. Onodera, S. Nara, A. Suzuki, M. Koyama, H. Tsuboi, N. Hatakeyama, H. Takaba, C.A. Del Carpio, M. Kubo, A. Miyamoto, Tribol. Online 3 (2008) 280.
[36] M. Kubo, M. Ando, S. Sakahara, C. Jung, K. Seki, T. Kusagaya, A. Endou, S. Takami, A. Imamura, A. Miyamoto, Appl. Surf. Sci. 223 (2004) 188–195.
[37] B.J. Delley, Chem. Phys. 113 (2000) 7756.
[38] S.H. Vosko, L. Wilk, M. Nusair, Can. J. Phys. 58 (1980) 1200.
[39] J.P. Perdew, K. Burke, M. Ernzerhof, Phys. Rev. Lett. 77 (1996) 3865.
[40] H. Weinberg, P. Merrill, Surf. Sci. 33 (1972) 493.
[41] N.B. Arboleda Jr., H. Kasai, W.A. Dino, H. Nakanishi, Jpn. J. Appl. Phys. 46 (2007) 4233.
[42] M. Calatayud, C. Minot, J. Phys. Chem. C 111 (2007) 6411.